



Investigating corrosion behavior and antibacterial properties of fluorohydroxyapatite coating on anodized Mg-2Zn-1.5Y 0.5Zr alloy

Ata Abednia

Bachelor in material and metallurgy engineering

Mohammad Hasan Rajabi Delivand

Bachelor in material and metallurgy engineering

Abstract

The research focuses on developing a biocompatible coating of fluorohydroxyapatite (FHA) with Tet213 peptide on a Mg-2Zn-1.5Y 0.5Zr alloy substrate through an anodizing process. The corrosion and antibacterial properties of the coating were examined, starting with the production of the alloy and anodizing it. FHA coatings with varying fluorine concentrations were deposited using an electrochemical method. The spherical FHA phase with high stability and low dissolution rate displayed excellent biocompatibility and protective qualities. Corrosion tests revealed that the FHA coating with 2 mmol of fluorine exhibited the lowest weight loss and current density, showcasing superior corrosion resistance. Increasing fluorine concentration led to the formation of bone-like hydroxyapatite with a structure conducive to bone cell growth. Incorporating Tet213 peptide enhanced the antibacterial properties, inhibiting biofilm formation and reducing the risk of infection at surgical sites. Ultimately, this innovative coating shows promise for medical applications requiring both corrosion resistance and antibacterial qualities.

Keywords: Magnesium alloy, fluorohydroxyapatite, electrochemical deposition, corrosion rate control, antibacterial property



Introduction

During the last decade, magnesium as a biodegradable biomaterial in the production of orthopedic implants has replaced common permanent metal biomaterials such as stainless steel, cobalt, titanium and its alloys [1, 2]. As an alkaline earth metal, magnesium is shiny and silvery white in appearance. It is also very reactive and is not found in free form in nature [3, 4]. Features such as biocompatibility and safety [5], presence in metabolic activities, density (1.74-2 grams per cubic centimeter) close to natural bone (1.8-2.1 grams per centimeter cubic meter), the modulus of elasticity (41-45 GPa) is close to that of natural bone (3-20 GPa), which prevents osteoporosis caused by the removal of normal stresses from the bones by the implant, and also stimulates cell growth. It has caused the attention of researchers to be drawn to the use of this metal in the production of orthopedic implants. However, the high corrosion rate in the body limits the use of pure magnesium [6-10]. Alloying and coating have been introduced as suitable solutions to overcome this problem and adapt the corrosion rate to the length of the treatment period [8, 11].

The elements used in magnesium alloying must be safe in the body. Therefore, among many elements, zinc and yttrium metals are among the best options. Kai and his colleagues [12], by examining different amounts of zinc in magnesium, found that magnesium containing 5% by weight of zinc has the best corrosion resistance in Mg-Zn binary alloys and its mechanical properties are also favorable. When the amount of yttrium element is 25% by mass, the hardness of the alloy reaches 119 HV, and its compressive strength increases to 417 MPa [13]. According to the research conducted by Jafari and his colleagues [14], in the Mg-5Zn alloy containing 0.7% by weight of Y, due to the presence of the secondary phase Mg₃Zn₆Y (I-phase) in the grain boundaries, the best corrosion resistance among the alloys containing up to It provides 1.5% by weight of Y. [15] But the corrosion rate is still higher than the required level, which makes it necessary to apply a biocompatible, biodegradable coating with proper adhesion. Hydroxyapatite is considered as a suitable coating due to its similarity to bone compounds [16-19]

Similar to other magnesium-zinc clay series alloys, its mechanical properties can be increased by heat treatment [20]. As a result, the required strength can be obtained by developing magnesium alloys [21].

According to the research results of Rad and his colleagues [22], adding fluorine to hydroxyapatite accelerates the process of cell growth; In fact, the combination of fluorohydroxyapatite (FHA) can create good protective conditions due to its lower dissolution rate and higher thermodynamic stability. It should be mentioned that the high reactivity of magnesium and its low melting point limit the use of multiple coating methods. However, the electrochemical deposition method is used as a simple and cheap method [23, 24]. The results of studies by Tan and his colleagues (25) show that by creating a porous substrate of magnesium hydroxide by anodizing method, the adhesion of the coating improves. In fact, the anodized layer acts as an intermediary between the coating and the base (26, 27). After applying the appropriate coating, it is very important to use an antibacterial compound; Because the infection caused by placing the implant in the tissue is considered as a big problem in medical surgeries and gram-negative bacteria (*P.aeruginosa*) act as the cause of wound and infection in the place where the implant is placed. (28). Common antibacterial compounds such as silver ion and titanium oxide, despite the power to destroy bacteria through the reaction between the released ions and bacteria, due to the limited antibacterial activity and biocompatibility of the released ion in the tissue, are facing a challenge. They are [29-31]. Therefore, researchers' efforts have led to the introduction of new types of antibacterial compounds. Peptides are a new example of antibacterial compounds that are compatible in the body and have long-term antibacterial activity. They destroy bacteria by penetrating the cell membrane and creating a pore, or after entering the cytoplasm, while inhibiting enzymes and intracellular reactions (32-34). Antibacterial peptides, despite having several specific mechanisms of action, generally do not face bacterial resistance (31, 35). Considering that antibacterial peptides have high biological activity and impose a much lower treatment cost on the patient, many researchers consider these compounds to be a suitable option for orthopedic applications; Also, the lack of side effects, low toxicity, lack of resistance to them, and a wide and fast spectrum of activity have made these compounds a suitable option for creating antibacterial properties on orthopedic implants without harming them. to the host tissue and having side effects on the biological function of the tissue (31-33). A large family of peptides based on origin, size, structure, amino acid sequence, biological function or reaction, mechanism of action, and. They are divided into different types. According to the results of research (28), Tet213, MX226, hIF1 and Tobramycin are the most famous new antibacterial peptides that have been used in the coating of orthopedic equipment; In the meantime, Tet213 peptide has a suitable function against gram-positive and gram-negative bacteria (28-32). Therefore, the aim of this research is to create a suitable coating of fluorohydroxyapatite by electrochemical deposition method and measure its adhesion on the anodized Mg-5Zn-0.7Y alloy, followed by investigating the corrosion behavior, the chemical composition of the corrosion product, and the surface morphology. eaten in the simulated body environment (SBF) and also studying the antibacterial properties and behavior of the Tet213 peptide in the culture medium of gram positive and negative bacteria

Materials and Methods

Materials preparation

To produce Mg-5Zn-0.7Y alloy, Amighan Mg-30Y, magnesium and zinc ingots with high purity (99.9%) were used. The raw materials were placed in a simple carbon steel crucible and in a resistance electric furnace (Azar furnaces-



VM10L1200, Iran) and were melted at a temperature of 780 degrees Celsius. In order to prevent the oxidation of the melt, argon gas was continuously blown in all stages of melting. The prepared melt was poured into a simple carbon steel mold that was preheated to a temperature of 420 degrees Celsius. The chemical composition of cast alloys was obtained using the Inductively Coupled Plasma (ICP) spectroscopy method. To conduct the research, a number of samples with dimensions of 20 mm x 15 mm x 10 mm were cut from ingots.

Processing of FHA coating on anodized Mg alloy surface

Samples with dimensions of 10mm x 10mm x 15mm were sanded using waterproof SiC sandpaper up to No. 2500. In the next step, surface preparation was completed with the help of diamond paste and polishing machine. Before applying the coating, an anodizing process was performed in order to increase the adhesion of the coating to the magnesium substrate. For this purpose, the cast alloy samples were degreased after preparation in a solution of 12% NaOH 12% Na₂B₂O₇.10H₂O 9% Na₂SiO₃ at a temperature of 75 degrees Celsius for 2-3 minutes and in Electrolyte bath containing 250 ml of 1wt% KOH 1.6wt% K₂SiO₃ solution as anode was anodized. Stainless steel was also used as a cathode. According to the research carried out by Shi and his colleagues [36] in order to achieve a fine and uniform coating and achieve proper adhesion, the anodizing process for a period of 30 minutes (in the first 10 minutes of a current density of 20 milliamperes per square centimeter, in the middle 10 minutes, the current density was set to 10 mA / cm², and in the last 10 minutes, the current density was 5 mA / cm². Then, the electrochemical deposition process was used to create FHA coating with different concentrations of fluorine (1, 1.5, and 2 mmol) on the anodized layer. In this method, two cells of graphite (anode) and anodized samples (cathode) were prepared. Then the electrolyte solution was prepared with the chemical composition of table (1). The constant current density was set equal to 20 milliamperes per square centimeter and the duration of the coating process was chosen to be 150 minutes. During the process, the electrolyte solution was circulating at a speed of 300 rpm.

Table 1- Materials and their consumption in the preparation of electrolyte solution

Dosage	Material
0.042mol/l	CaNO ₃
0.025 mol/l	NH ₄ H ₂ PO ₄
0.15 mol/l	NaNO ₃
20 ml	H ₂ O ₂
1, 1.5 , 2 mmol/l	NaF
2g/l	Na ₃ PO ₄

Characterization of coat on anodized Mg alloy

After applying the FHA coatings on the anodized samples, and washing them with deionized water, scanning electron microscopic studies (SEM, MIRA3 TESCAN) from the surface of the coating to The purpose of examining the morphology and cross-sectional area of the sample to determine the thickness and uniformity of the coating along with X-ray energy diffraction spectroscopy (EDS) and X-ray diffraction analysis (XRD, JEDL, JDX-8030), to determine the chemical composition and phases in The coverage was done.

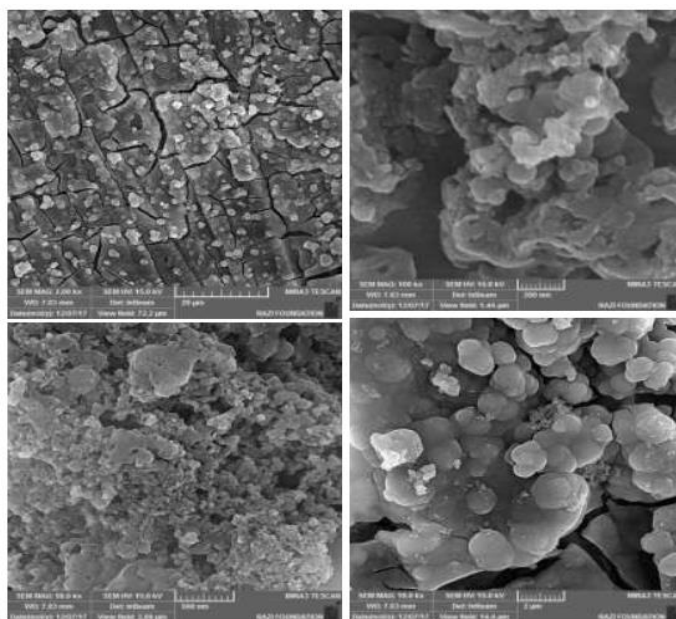


Figure 1- Scanning electron microscopic images of the surface of the coating layer on the magnesium substrate

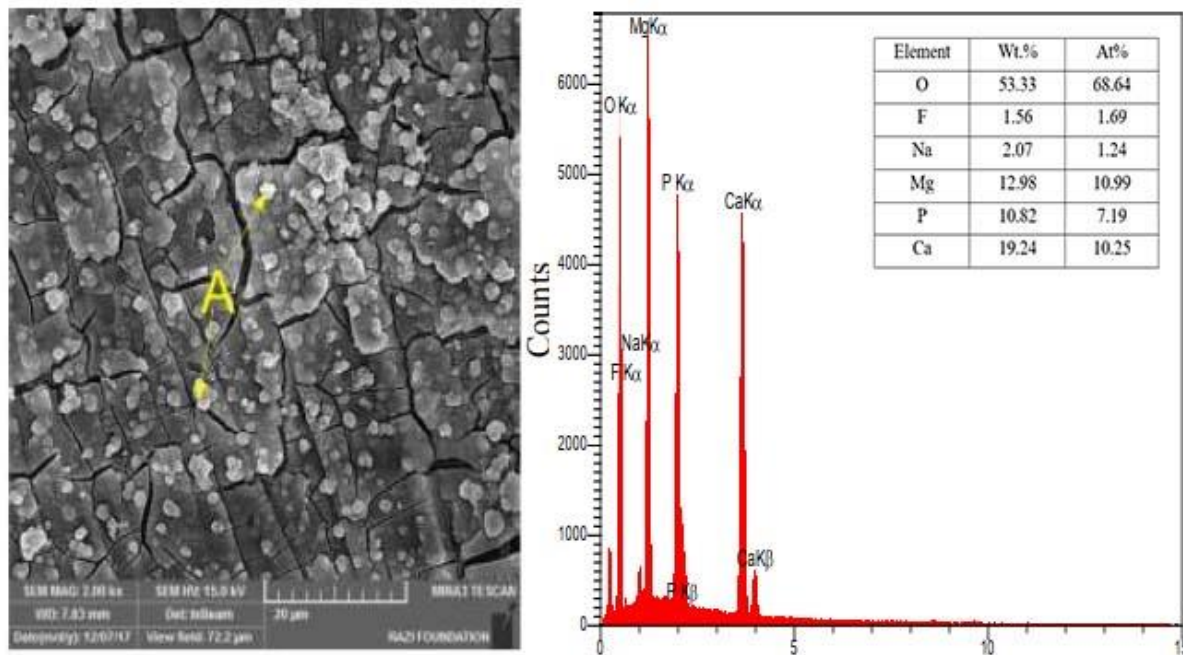


Figure 2- Spot EDS results of fluorohydroxyapatite coating on magnesium substrate

Electrochemical tests

The corrosion behavior of coated and uncoated alloys was investigated by immersion and polarization tests in SBF solution with a pH of 7.40 and a temperature of 37°C. The immersion test was performed according to the ASTM G31-72 standard; In this order, the samples were placed in the SBF solution for 168 hours after being washed and weighed by a digital scale with an accuracy of 0.0001 grams. The samples were removed from the solution every 24 hours, the corrosion products were removed using 180 g / l chromic acid without damaging the sample, and after washing with hot distilled water, they were dried in a stream of hot air. And then their weight was recorded. The pH of the solution containing the samples was also measured every 24 hours by a pH meter (SANA SL-901). It should be noted that in order to obtain reliable results, three samples of each coating were examined and the average weight loss was reported and the corrosion rate was determined using equation [1-3].

$C.R = W \times k / A \times T \times D$ relationship (1-1)

In this relation, $k = 8.76 \times 10^4$, W is the amount of weight loss (grams), A is the cross-sectional area of the sample in contact with the solution (square centimeters), T is the immersion time (hours), and D is the density of the sample (grams per cubic centimeter)

The polarization test was carried out with the aim of completing the corrosion test and in order to investigate the corrosion behavior of the coatings, using the Autolab device (model PGSTAT302N). The coated samples were placed as working electrodes in a three-electrode cell containing 500 ml of SBF solution. calomel reference electrode (SCE) and platinum electrode were added to the cell set as counters. By setting the voltage range between -2.5 and -1.5 V (relative to OCP) and scanning speed of 0.5 mV / s, the polarization test was performed. The resulting curves (voltage according to corrosion current density) were obtained by NOVA software. With the help of TOEFL slope, current density and corrosion potential were determined and corrosion rate was calculated.

Peptide loading on coated Mg alloy

Tet213 peptide with a short amino acid length (9 amino acids) with a C terminal chain (KRWKWWRRRC) was investigated as a new antibacterial substance in this research. The loading process of this peptide includes creating a solution of 50 mmol of sodium hydrogen phosphate in distilled water, which is obtained by using 0.1 M sodium hydroxy solution, a suitable pH of 7.4. This solution is poured into a small glass container; 1 ml of this buffer is added to a glass container containing 1 mg of peptide; Then the alloy samples are coated and immersed in room temperature for 1 hour. After that, the samples are washed 10 times with distilled water, each time for 1 minute. Washing in distilled water provides the highest peptide concentration. After washing, the samples are exposed to air with a slow flow to dry. (20)

Immobilized Peptide detection

The amount of peptide on the surface of the samples is estimated by fluorometric technique. After dissolving the coating in 1 ml of 0.1 M hydrochloric acid solution for 1 hour in an ultrasonic bath, 3 ml of PHQ reagent is added to it. Then, the contents of the glass container are transferred to a water bath with a temperature of 30 degrees centigrade. After 3 hours, the reagent reacts with the residue of the tested peptide. The combined reaction solution has fluorescence properties. To stop the reaction, 2.25 ml of 2.4 M hydrochloric acid solution is added. The amount of peptide is estimated based on amino acid concentration by luminometric method [28].

Antibacterial activity testing

Antibacterial activity against both Gram-positive (*S. aureus*) and Gram-negative (*P. aeruginosa*) bacteria is investigated. At the beginning, both types of bacteria are cultured overnight. 100 microliters of each bacterial solution was poured into sterile tubes containing 5 ml of Mueller Hinton Broth (MHB) and kept at 37°C for 1 hour. Then the bacterial suspension is suspended by Basal Medium 2 (BM2) or (MHB) until the final density is 106 cells/mL. 400 microliters of gram-positive or gram-negative bacterial suspension is dripped separately on three samples of coated alloy containing peptide. After 30, 90, 150 and 270 minutes of soaking with gram-positive or gram-negative bacterial suspension, the remaining bacteria (residue) on the sample covered by nutrient agar and overnight at room temperature. It is kept at 37°C to estimate the survival rate of the bacteria by counting the number of colony forming units (CFU). In microbiology, a colony forming unit (CFU) is a unit used to estimate the number of bacterial cells in a sample. In order to count the colony formation units, it is necessary to grow the bacteria in the culture medium first. In this method, unlike the microscopic method in which both dead and living cells are counted, only living cells are counted. Open CFU counting software was also used for accurate counting. For this purpose, a photo was taken of the plate where the colonies were grown. By submitting this photo to colony counting software, their number was obtained. Bacteria sensitivity to Tet 213 peptide is evaluated by preparing 6 FHA-AMP samples. In this way, the samples are kept at a temperature of 37 degrees Celsius for 4, 24 and 48 hours, and the sensitivity of the bacteria is measured by the decrease in bacterial luminescence; This is a quick technique for measuring bacteria and microorganisms using a special reagent, which is reported as the percentage of sensitivity to the luminescence value of untreated bacteria. Since the direct measurement of the amount of peptide released from the samples is the main problem, the antibacterial test indirectly estimates the antibacterial effect. 6 samples of FHA-AMP are placed in contact with *P. aeruginosa* bacteria for 30 minutes. The bacterial solution is removed by a pipette and the samples are washed 3 times with a buffered phosphate salt solution. Then the samples are dried in the air, after that they are treated with equal amounts of bacteria for another 30 minutes; After the CFU test was performed as described above. The antibacterial activity cycle is performed for 4 consecutive times to determine the antibacterial activity [28].

Results and discussion

According to the scanning electron microscopic image of the surface of the anodized layer, this layer is porous, which can be seen with a dark color in the figure, and it has a diameter of about one micron. These pores increase the adhesion to the main coating. The anodic reaction of anodizing magnesium dissolution is always accompanied by the cathodic decomposition of water, which leads to the production of molecular hydrogen. Of course, the production rate of this gas depends on the magnesium-based alloy, and in case of accumulation near the medical implant, it must be discharged, which is a proof of the necessity of applying the coating on the anodized substrate.[37-39]

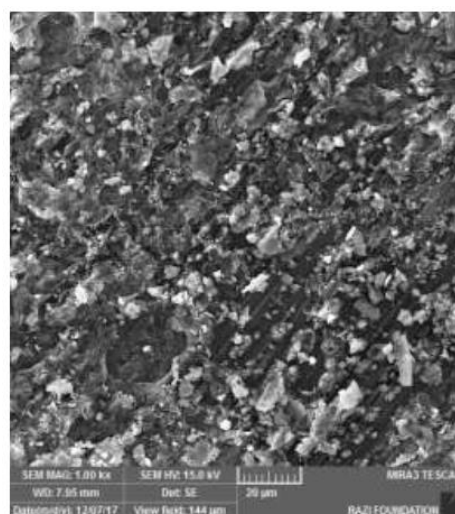


Figure3- Scanning electron microscopic image of the surface of the anodizing layer

Analysis of coating

Figure 4 shows the scanning electron microscopic images of the FHA coating applied on the anodized magnesium alloy in different concentrations of fluorine. As can be seen, in general, the resulting coating consists of a dark background of cracked and desert-shaped magnesium hydroxide and white particles of fluorine and hydroxyapatite with spherical morphology. This coating with a spherical structure has a good resemblance to bone compounds. This type of spherical morphology, compared to the plate morphology seen in other calcium-phosphate coatings, creates better conditions for the absorption of calcium and phosphate ions in the body solution, and therefore It will help the growth of new bone cells in the damaged area[22]. According to Figure 4, it can be predicted that the phase of fluorine and bone-like hydroxyapatite increased by increasing the amount of fluorine element in the coating; In such a way that the image (a) includes the dark background of magnesium hydroxide and the presence of white particles of fluorine and hydroxyapatite in a small amount can be seen on it.

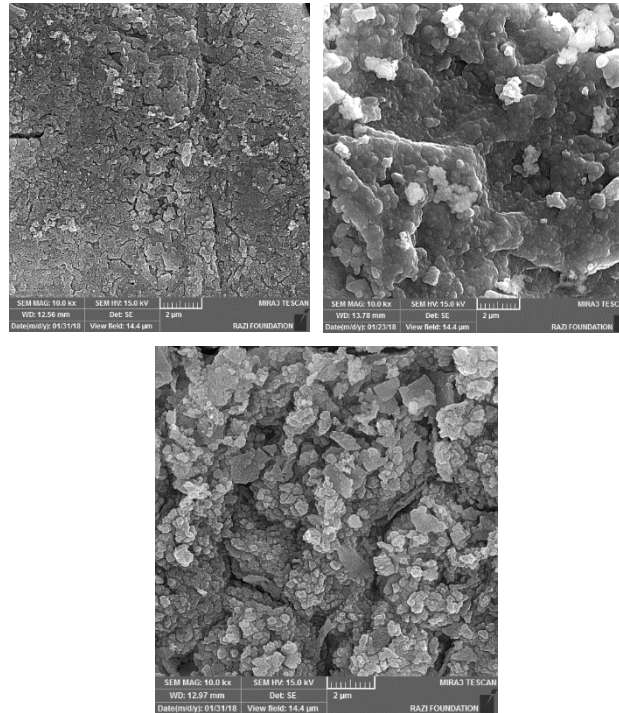


Figure 4 - Scanning electron microscope images of the surface of the coatings obtained from the solution containing: (a) 1 mmol, (b) 1.5 mmol and (c) 2 mmol of fluorine

By increasing the percentage of fluorine to 1.5 mmol, the white spherical particles of fluorine and hydroxyapatite increase (picture (b)) so that with the further increase of fluorine to 2 mmol, the coating of a piece of The spherical particles of fluorine and hydroxyapatite can be seen on the pores of the anodizing layer (picture (c)), which provides far better conditions for the absorption of calcium ions, phosphate and bone cells after Being in SBF provides; In other words, it shows a good correlation with the bone. Therefore, according to the results of the scanning electron microscope, it can be acknowledged that the coating containing 2 mmol of fluorine is more biocompatible and suitable for medical applications, especially orthopedic implants [23].

Figure 5 shows the EDS results of the coatings shown in Figure 1, which indicates the presence of oxygen, magnesium, fluorine, calcium, phosphorus, and zinc elements in all three coating samples, which indicates the presence of magnesium hydroxide phases and fluorohydroxy phase. It is uptime. According to the quantitative results, it can be seen that not only the increase of fluorine has led to the increase of this element in the coating, but also the Ca/P ratio from 1.22 for 1 mmol to 1.38 for 1.5 mmol and 1.47 increased for 2 mmol of fluorine. It is important to mention that a higher Ca/P ratio indicates that the hydroxyapatite phase is richer in calcium, which creates the conditions for higher solubility and, as a result, the creation of more bone cells on the metal implant after its placement. It provides in the host tissue. Therefore, the increase of fluorine causes the qualitative and quantitative improvement of the fluorine phase and hydroxyapatite formed in the coating, which provides a suitable option for coating medical equipment.

Figure 6 shows the XRD test results of all 3 coatings. X-ray diffraction patterns indicate the presence of $Mg(OH)_2$ and FHA phases, which confirms the analysis of EDS results. The patterns in Figure 3 also show that with the increase in the percentage of fluorine, the peaks related to the FHA phase become more intense; In addition, the presence of fluoroapatite (FA) phase has also been reported in small amounts. This phase with the chemical composition of $Ca_5(PO_4)_3F$ and needle morphology is one of the biocompatible minerals found naturally and in small amounts in



the mineral tissues of the body. It should be noted that the presence of this phase can reduce the current density and corrosion potential in SBF [41]. This phase, along with the fluorohydroxyapatite phase in the biological environment of the body, causes: faster formation of bone-like apatite (biological mineralization process), better absorption of protein and bone-forming cells on the surface, lower dissolution rate, higher chemical stability. , improving mechanical properties, higher corrosion resistance, improving cell attachment and cell proliferation rate [42, 43]. Therefore, it will have very suitable conditions for covering orthopedic implants. In the third coating, the fluorine peak corresponding to fluorohydroxyapatite is reinforced with a higher amount and it is expected to provide suitable conditions in terms of biocompatibility and is a suitable option for coating medical equipment.

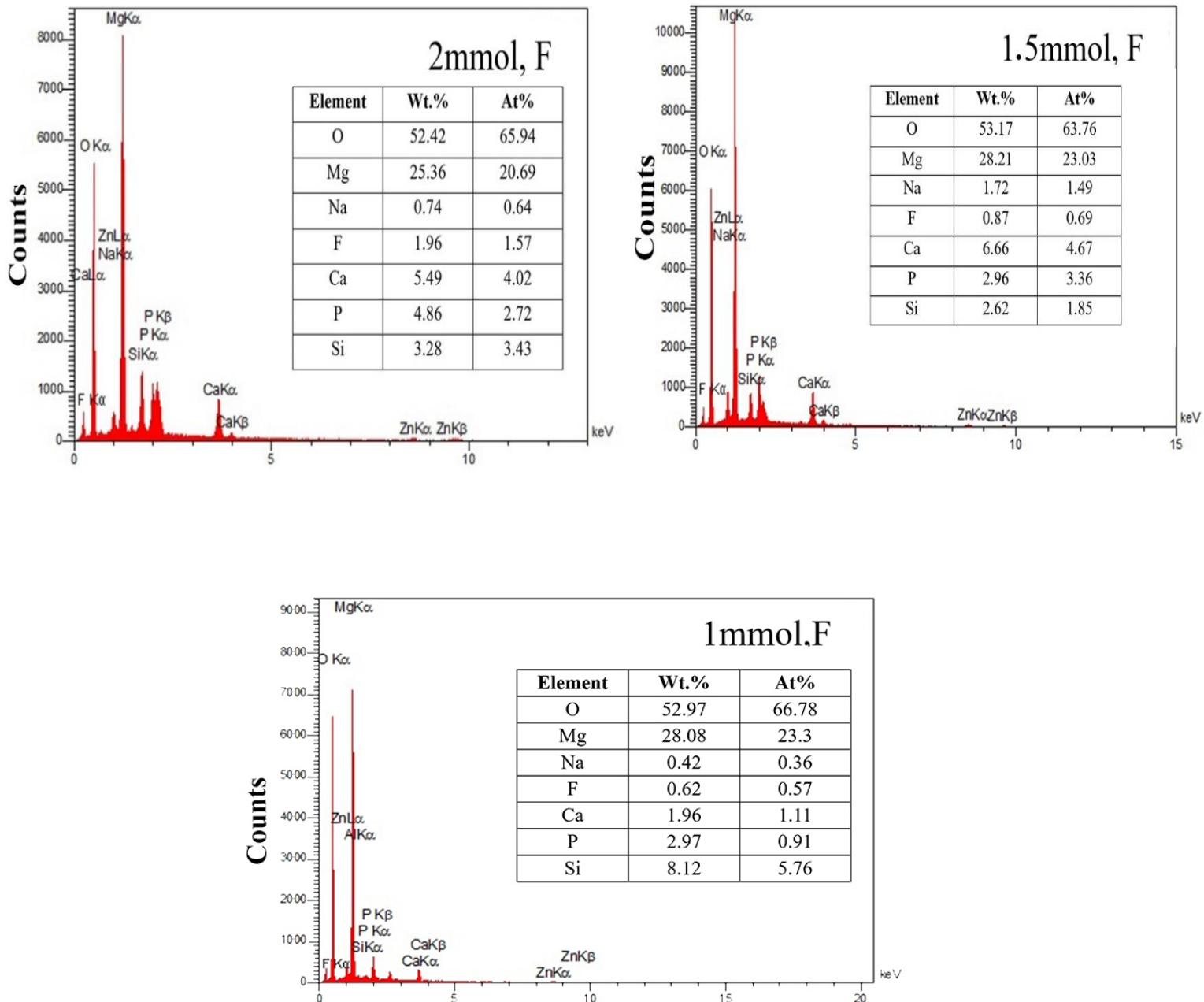


Figure 5- EDS test results of three samples of fluorine and hydroxyapatite coating on anodizing substrate

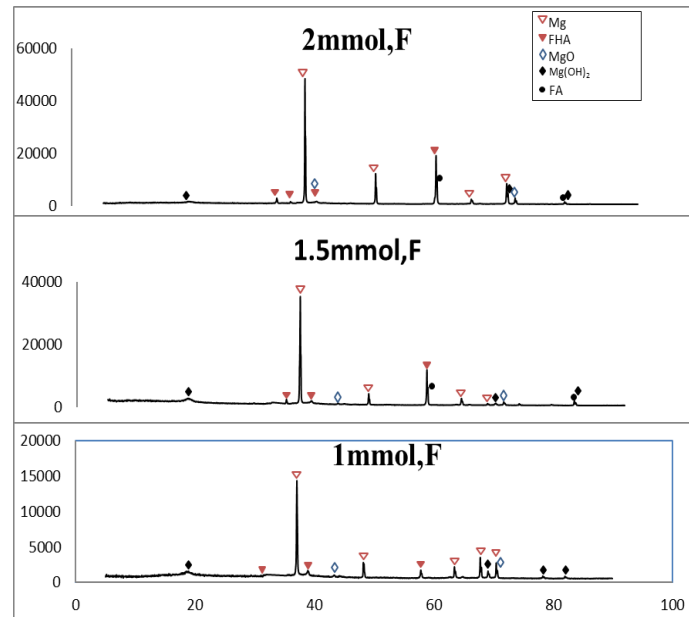


Figure 6- X-ray diffraction patterns of coatings

Electrochemical measurement

Immersion test

Figure 7 shows the weight loss graph of Mg-2Zn-1.5Y 0.5Zr samples without coating and coated with fluorohydroxyapatite with different concentrations of fluorine. For the uncoated sample, we see a greater weight loss, which is caused by pitting corrosion in the porous magnesium hydroxide film in the presence of chlorine ions. For this reason, the mentioned film cannot play the role of sufficient protection from the base alloy. But the application of fluorohydroxyapatite coating has been able to significantly reduce the amount of weight loss. As this graph shows, after 168 hours of SBF immersion, the coating obtained from the solution containing 1 mmol of fluorine, caused a decrease of 12.7% in the weight loss of the sample compared to the sample without coating. In the same way, with the increase of fluorine to 1.5 and 2 mmol, respectively 12 and 11.5 percent decrease in the amount of weight loss of the samples can be seen. The reason for this performance in weight loss is due to the presence of fluorine ion. Substitution of fluorine ion instead of hydroxyl group causes a significant reduction in the corrosion rate. On the other hand, the fluorohydroxyapatite coating has a structure with high thermodynamic stability and low dissolution and provides suitable conditions for the protection of the base metal [14].

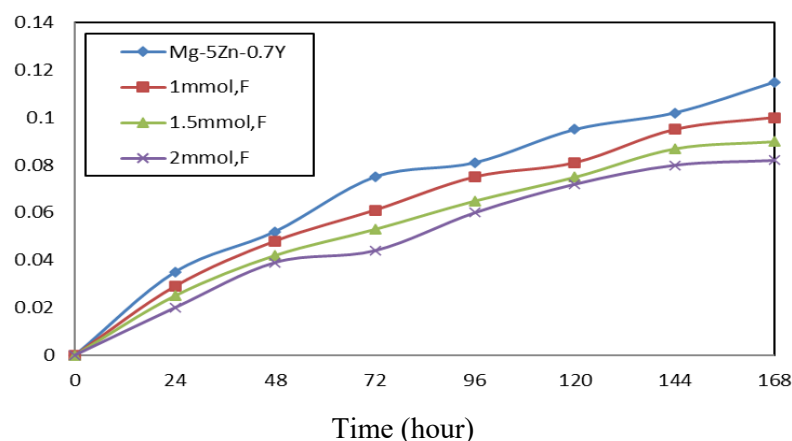


Figure 7- Weight loss graph of samples after 168 hours of immersion in SBF

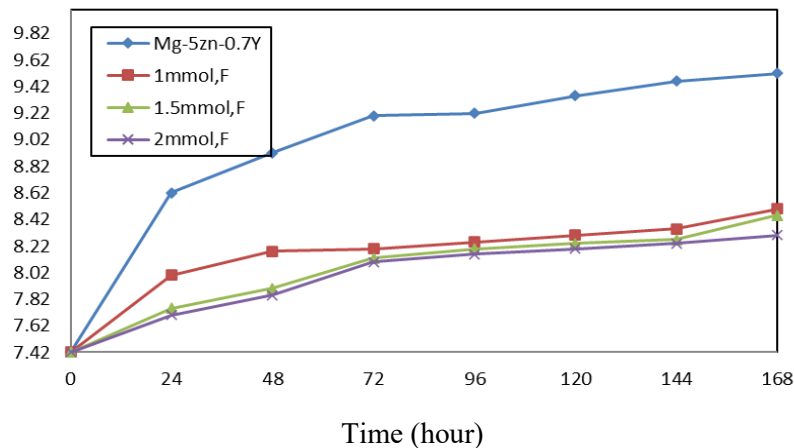


Figure 8- Graph of pH changes of samples after 168 hours of immersion in SBF

Figure 8 shows the graph of pH changes for all 4 samples. As can be seen in the figure, for all 4 samples, both uncoated and coated, a similar trend for pH changes can be seen. This process includes a rapid increase in pH in the early hours, although this is more for the uncoated sample, its proof is in the middle hours and finally its increase in the last hours of immersion. In other words, in the early hours due to high corrosion and the occurrence of anodic (reaction 1) and cathodic (reaction 2) reactions, the pH will increase sharply and hydrogen gas will be emitted. The presence of hydroxyl ion (OH^-) increases the pH values, but with its consumption by magnesium and the production of $\text{Mg}(\text{OH})_2$ (reaction 3), the graph reaches a constant slope.

- (1) $\text{Mg(s)} \rightarrow \text{Mg}^{2+}(\text{aq}) + 2\text{e}^-$: anodic reaction
- (2) $2\text{H}_2\text{O}(\text{aq}) + 2\text{e}^- \rightarrow \text{H}_2(\text{aq}) + 2\text{OH}^-(\text{aq})$: cathodic reaction
- (3) $\text{Mg}^{2+}(\text{aq}) + 2\text{OH}^-(\text{aq}) \rightarrow \text{Mg}(\text{OH})_2(\text{s})$: general reaction

It should be noted that in the case of the uncoated sample, the formation of $\text{Mg}(\text{OH})_2$ on the surface and the absence of the coating, and on the other hand due to the porosity of the hydroxide layer and the penetration of the electrolyte, the chlorine ions (Cl^-) present in the SBF solution, They cause pitting corrosion, as a result of which, $\text{Mg}(\text{OH})_2$ decomposes into MgCl_2 . During this reaction, with the occurrence of pitting corrosion, numerous holes are created on the surface of the sample, and therefore the increasing trend of pH is more than the coated samples. This is a proof of the lack of protection of the hydroxide layer as a corrosion product of basic magnesium. Therefore, with the occurrence of pitting corrosion reaction, OH^- is released and the pH rises. The presence of hydroxyl ion OH^- along with phosphate ions, HPO_4^{2-} , H_2PO_4^- and PO_4^{3-} and calcium ion Ca^{2+} provides the conditions for the formation of white hydroxyapatite particles (reaction 4) on the surface of the sample. The formation of hydroxyapatite ($\text{Ca}_{10}(\text{PO}_4)_6(\text{OH})_2$) and consumption of hydroxyl ion is a factor for reducing the rate of corrosion reaction and thus reducing the increasing trend of pH [7].

- (4) $\text{PO}_4^{3-} + 6\text{OH}^- + 10\text{Ca}^{2+} \rightarrow \text{Ca}_{10}(\text{PO}_4)_6(\text{OH})_2 + 10\text{Ca}^{2+} + 2\text{OH}^-$

Of course, it is important to mention that the hydroxyapatite formed in the uncoated sample does not have a good structural order due to its coarseness and high formation rate, and on the other hand, due to the lower Ca/P ratio, it dissolves sooner. It is important to mention that this combination causes the absorption and proliferation of bone cells to some extent, but its time does not correspond to the length of the treatment period, and this makes it necessary to apply the coating. In the case of coated samples, the pH values change during immersion times similar to the uncoated sample; To the part that in the early stages of the immersion test, due to the release of OH^- and the decomposition of the coating, the pH increased steeply and then reached equilibrium. This equilibrium occurs due to the penetration of the solution at the interface of FHA and the base through the pores and cracks of the corroded coating in SBF. The precipitation of apatite that consumes OH^- ions is another reason for increasing the pH in the final stages. In the case of the FHA coating resulting from the solution containing 2 mmol of fluorine, the rate of increase is lower; In other words, replacement of OH^- ion with F^- in the structure of apatite leads to a dramatic decrease in the dissolution rate of apatite in SBF. On the other hand, fluorine ion prevents the pitting corrosion of magnesium hydroxide by chlorine and reduces the corrosion rate. slow -Hydroxyapatite, through the absorption of phosphate and calcium ions, takes place at a more favorable rate in the presence of fluorine ion, and it has a better structural order

and is thermodynamically stable, so it can better absorb and multiply cells. perform a bone according to the length of the treatment period [22, 23].

Polarization test

Figure 9 shows the polarization curves for samples coated with different concentrations of fluorine. Using TOFEL slope, current density and corrosion potential of the mentioned samples are given in Table 2. By adding 1, 1.5, and 2 mmol of fluorine, the current density was obtained as 19.2, 12.9, and 10.1 microamps per square centimeter, respectively. In fact, the presence of fluorine causes the formation of a protective layer and limits the ion transfer reaction, and ultimately increases the corrosion resistance [22]. It can be acknowledged that fluorohydroxyapatite has a dense corrosion layer compared to other calcium-phosphate compounds. It provides more and more uniformity. In the case of the coating obtained from the solution containing 2 mM fluorine, the better structure has improved the corrosion resistance. The polarization curves of all three coating samples are similar, indicating that the electrochemical reactions and the corrosion mechanism are the same. The presence of a long passive zone for all three coated samples indicates a decrease in the corrosion current density due to the presence of fluorohydroxyapatite particles. Unlike the current density and corrosion rate, the corrosion potential did not change as expected. The results of this test also confirm the results of the immersion test.

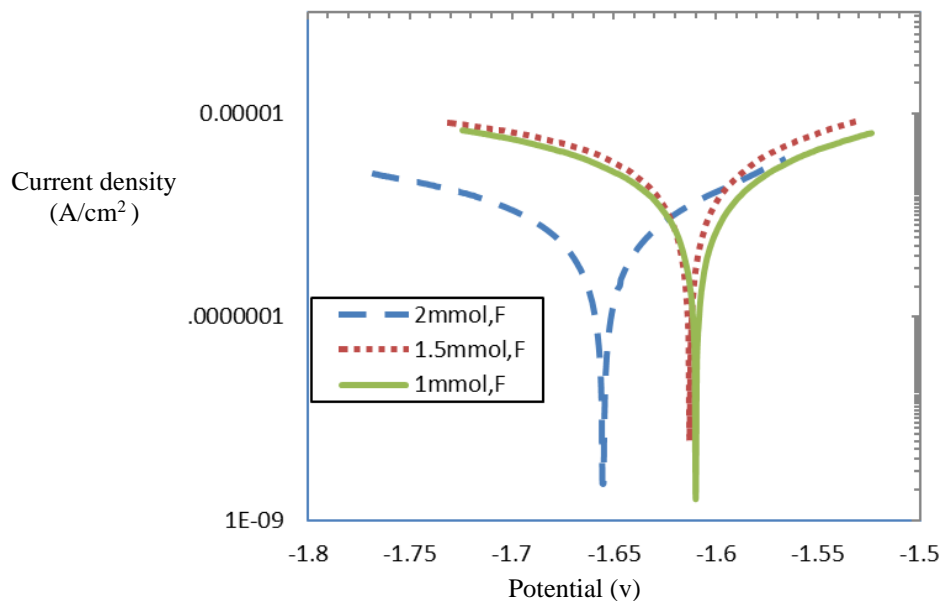


Figure9- Polarization curves of samples coated in SBF

The chemical composition of the corrosion product and the morphology of the corroded surface

Figure 10 shows the SEM images of the corroded surfaces of the samples coated with fluorohydroxyapatite containing different amounts of fluorine.

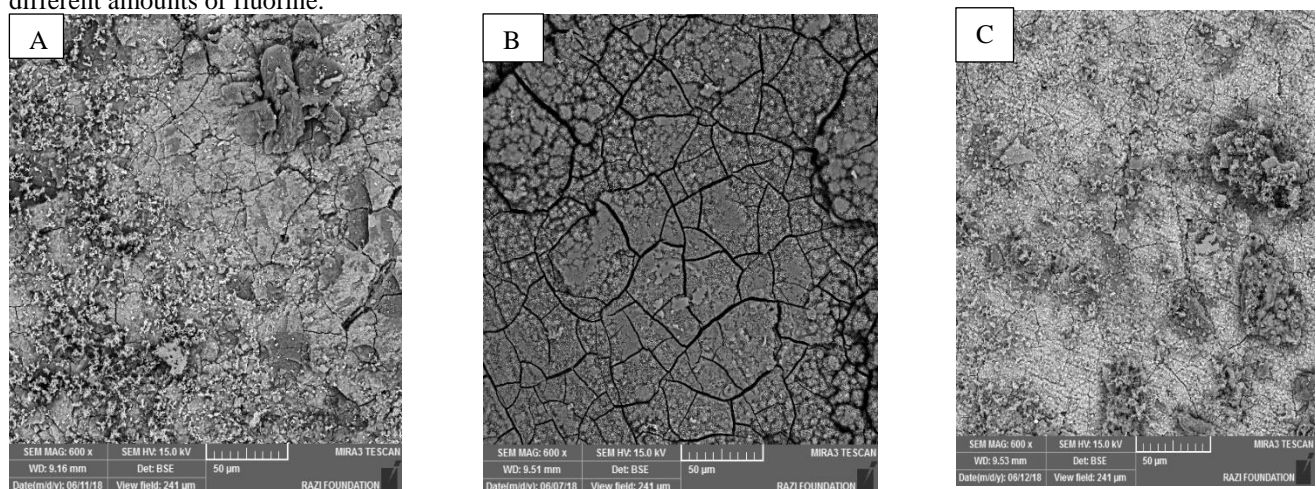


Figure 10- Images of corroded surfaces of fluorohydroxyapatite coating samples containing: a) 1 mmol, b) 1.5 mmol and c) 2 mmol of fluorine.



Also, these images show that the corrosion products formed on the fluorohydroxy-apatite coating have a dense and uniform structure. In the corrosion products, there are holes with very small dimensions in the nano range. As mentioned earlier, the presence of fluorine ion, while increasing biocompatibility and bioactivity, helps to form bone-like hydroxyapatite and, subsequently, create new bone cells in the damaged area. It does [45, 46]. The researchers are of the opinion that the fluorine ion present in the electrolyte and the coating creates a stable hydroxyapatite, which will cause the desire for more suitable corrosion properties and adapt the repair of the damaged tissue to the length of the treatment period [47].

Conclusion

1. The application of fluorohydroxyapatite coating with concentrations of 1, 1.5 and 2 mmol on the anodized substrate has been well done due to the presence of the porous magnesium hydroxide substrate, in such a way that, while improving the adhesion properties, a coating with uniformity and appropriate density has been created. which will be able to create the desired protective effect due to low solubility rate and high thermodynamic stability.
2. In relation to the created cover, write a result according to the experiments.
3. By increasing the concentration of fluorine from 1 to 1.5 and then to 2 mmol, the formation of the fluorohydroxyapatite phase with finer cellular structure on the magnesium alloy is improved quantitatively and qualitatively. Also, increasing the concentration of fluorine, increasing the ratio of Ca/P will lead to the formation of calcium-rich FHA coating, which will improve the absorption and growth of bone cells.
4. The antibacterial property of the coating was obtained by applying the Tet213 peptide with a long-term effect, biocompatibility and higher bone cell growth compared to conventional antibacterial compounds.
5. The concentration of a significant amount of Tet213 peptide on the surface of the coating results in the complete destruction of bacteria in the bacterial culture medium and indicates the proper inhibition of its bacterial growth. Also, the long-term effect of this substance is to prevent the creation of biofilm and, of course, infection and wound in the tissue around the implant.

References

1. Song G. Control of biodegradation of biocompatible magnesium alloys. Corrosion science. 2007;49(4):1696-701.
2. Davis R, Singh A, Jackson MJ, Coelho RT, Prakash D, Charalambous CP, et al. A comprehensive review on metallic implant biomaterials and their subtractive manufacturing. The International Journal of Advanced Manufacturing Technology. 2022;120(3-4):1473-530.
3. Shand M. The chemistry and technology of magnesia. A John Wiley & Sons. Inc Publication. 2006.
4. Dobrzański LA, Totten GE, Bamberger M. The importance of magnesium and its alloys in modern technology and methods of shaping their structure and properties. Magnesium and its alloys: CRC Press; 2019. p. 1-28.
5. Istrate B, Munteanu C, Băltau M-S, Cimpoeșu R, Ioanid N. Microstructural and Electrochemical Influence of Zn in MgCaZn Biodegradable Alloys. Materials. 2023;16(6):2487.
6. Virtanen S. Biodegradable Mg Alloys: Corrosion, Surface Modification, and Biocompatibility. Biomedical Applications: Springer; 2012. p. 101-25.
7. Poinern GEJ, Brundavanam RK, Fawcett D. Nanometre scale hydroxyapatite ceramics for bone tissue engineering. American Journal of Biomedical Engineering. 2013;3(6):148-68.
8. Wu G, Gong L, Feng K, Wu S, Zhao Y, Chu PK. Rapid degradation of biomedical magnesium induced by zinc ion implantation. Materials Letters. 2011;65(4):661-3.
9. Zhang S, Li J, Song Y, Zhao C, Zhang X, Xie C, et al. In vitro degradation, hemolysis and MC3T3-E1 cell adhesion of biodegradable Mg–Zn alloy. Materials Science and Engineering: C. 2009;29(6):1907-12.
10. Hashemi M, Alizadeh R, Langdon TG. Recent advances using equal-channel angular pressing to improve the properties of biodegradable Mg–Zn alloys. Journal of Magnesium and Alloys. 2023.
11. Mehta S, Singh G, Saini A, editors. State-of-art of biomaterial coatings for enhanced biofunctionality of metallic implants. AIP Conference Proceedings; 2022: AIP Publishing.
12. Cai S, Lei T, Li N, Feng F. Effects of Zn on microstructure, mechanical properties and corrosion behavior of Mg–Zn alloys. Materials Science and Engineering: C. 2012;32(8):2570-7.
13. Wang M, Xiao D, Zhou P, Liu W, Ma Y, Sun B. Effects of rare earth yttrium on microstructure and properties of MgAlZn alloy. Journal of Alloys and Compounds. 2018;742:232-9.
14. Jafari H, Rahimi F, Sheikhsofla Z. In vitro corrosion behavior of Mg-5Zn alloy containing low Y contents. Materials and Corrosion. 2016;67(4):396-405.
15. Jafari H, Rahimi F, Sheikhsofla Z, Khalilnezhad M. Effect of Minor Yttrium on Microstructure and Mechanical Properties of Bioimplant Mg-5Zn Alloy. Journal of Materials Engineering and Performance. 2017;26:5590-8.



16. Williams DF. On the mechanisms of biocompatibility. *Biomaterials*. 2008;29(20):2941-53.
17. Rivera-Muñoz EM. Hydroxyapatite-based materials: synthesis and characterization. *Biomedical Engineering-Frontiers and Challenges*. 2011:75-98.
18. Elkayar A, Elshazly Y, Assaad M. Properties of hydroxyapatite from bovine teeth. *Bone and Tissue Regeneration Insights*. 2009;2:BTRI. S3728.
19. Li J, Song Y, Zhang S, Zhao C, Zhang F, Zhang X, et al. In vitro responses of human bone marrow stromal cells to a fluoridated hydroxyapatite coated biodegradable Mg–Zn alloy. *Biomaterials*. 2010;31(22):5782-8.
20. Li S, Dong X, Guo S, Ma R, Xiang D, Lü S, et al. Phase evolution and strengthening mechanisms in a cast magnesium-zinc-yttrium-zirconium alloy following different heat treatments. *Journal of Materials Research and Technology*. 2023;22:3270-9.
21. Hu J, Wan D, Hu Y, Wang H, Jiang Y, Xue Y, et al. A hysteretic loop phenomenon at strain amplitude dependent damping curves of pre-strained pure Mg during cyclic vibration. *Journal of Alloys and Compounds*. 2021;886:161303.
22. Rad HRB, Idris MH, Kadir MRA, Farahany S. Microstructure analysis and corrosion behavior of biodegradable Mg–Ca implant alloys. *Materials & Design*. 2012;33:88-97.
23. Ghayad I, Shoeib M, Girgis N, Soliman H, Abd El Hallem S. Effect of Surface Active Agents on the Performance of Hydroxiapatite Coating Electrodeposited on Mg-3 Zn-0.8 Ca Alloy.
24. Rončević IŠ, Grubač Z, Metikoš-Huković M. Electrodeposition of hydroxyapatite coating on AZ91D alloy for biodegradable implant application. *International Journal of Electrochemical Science*. 2014;9(11):5907-23.
25. Tan A, Soutar A, Annergren I, Liu Y. Multilayer sol–gel coatings for corrosion protection of magnesium. *Surface and coatings technology*. 2005;198(1-3):478-82.
26. Nassif N, Ghayad I. Corrosion protection and surface treatment of magnesium alloys used for orthopedic applications. *Advances in Materials Science and Engineering*. 2013;2013.
27. J. Gazapo aJG. . Anodizing of Aluminum. TALAT Lecture 5203. 1994;European Aluminum Association:27 pages.
28. Kazemzadeh-Narbat M, Kindrachuk J, Duan K, Jenssen H, Hancock RE, Wang R. Antimicrobial peptides on calcium phosphate-coated titanium for the prevention of implant-associated infections. *Biomaterials*. 2010;31(36):9519-26.
29. Yan YC. Antibacterial properties and Biocompatibility of Novel Peptide Incorporated Titanium Alloy Biomaterials for Orthopaedic Implants. Degree of Master of philosophy of The university of Hong kong. 2010;(pp.60-63).
30. Bosco R, Van Den Beucken J, Leeuwenburgh S, Jansen J. Surface engineering for bone implants: a trend from passive to active surfaces. *Coatings*. 2012;2(3):95-119.
31. L. Wang JC, L. Shi, L. Ren, Y. Wang. The promotion of Antimicrobial Activity on silicon substrates by A immobilized short peptide. *Electronic Supplementary Materials for chemical Communications*. 2013;Vol.2:(pp. 13-7).
32. M. Saderdinamin FM, P. Hosseini, F. Doustidar. Antimicrobial Peptides. *Novelty in Biomedicine*. 2015;Vol. 4(No.2):(pp. 70-6).
33. Cézard C, Silva-Pires V, Mullié C, Sonnet P. Antibacterial peptides: A review. *Science against Microbial Pathogens: Communicating Current Research and Technological Advances: Formatex Research Center*. 2011.
34. Phoenix DA, Dennison SR, Harris F. *Antimicrobial Peptides*: John Wiley & Sons; 2012.
35. Jangir PK, Ogunlana L, Szili P, Czikkely M, Shaw LP, Stevens EJ, et al. The evolution of colistin resistance increases bacterial resistance to host antimicrobial peptides and virulence. *Elife*. 2023;12:e84395.
36. Z. Shi GS, A. Atrens. Influence of anodizing current on the corrosion resistance of anodized AZ91D magnesium alloy. *Corrosion Science*. 2006;Vol.48:(pp. 1939-59).
37. E.Strazzi CF. Low energy consumption and Environmental friend
process for magnesium anodizing. *Low energy*. 2012; Vol.1 (pp.5-8).
38. M.K. Sharma YJ, J. Kim, H. Kim and J.P. Jung Plasma
Electrolytic oxidation in surface Modification of metals for Electronics. *Journal of welding and joinig*. 2014;Vol.23. No.2:(pp. 30-24).
39. S.A. Salman RM, R. Ichino, M. Okido. . Effects of Anodising Potential on the surface Morphology and Corrosion Property of AZ31 Magnesium Alloy. *Materials Transactions*. . 2010;Vol.51. No.6:(pp. 1109-13)
40. Chai L, Yu X, Yang Z, Wang Y, Okido M. Anodizing of magnesium alloy AZ31 in alkaline solutions with silicate under continuous sparking. *Corrosion Science*. 2008;50(12):3274-9.
41. Yang Y, Lu C, Shen L, Zhao Z, Peng S, Shuai C. In-situ deposition of apatite layer to protect Mg-based composite fabricated via laser additive manufacturing. *Journal of magnesium and alloys*. 2023;11(2):629-40.



42. Fattah-alhosseini A, Chaharmahali R, Alizad S, Kaseem M. Corrosion behavior of composite coatings containing hydroxyapatite particles on Mg alloys by plasma electrolytic oxidation: A review. *Journal of Magnesium and Alloys*. 2023.
43. Tredwin CJ, Young AM, Abou Neel EA, Georgiou G, Knowles JC. Hydroxyapatite, fluor-hydroxyapatite and fluorapatite produced via the sol-gel method: Dissolution behaviour and biological properties after crystallisation. *Journal of Materials Science: Materials in Medicine*. 2014;25:47-53.
44. Seyedmajidi S, Seyedmajidi M. Fluorapatite: A Review of Synthesis, Properties and Medical Applications vs Hydroxyapatite. *Iranian Journal of Materials Science & Engineering*. 2022;19(2).
45. Wang M, Zhang H-Y, Xiang Y-Y, Qian Y-P, Ren J-N, Jia R. How does fluoride enhance hydroxyapatite? A theoretical understanding. *Applied Surface Science*. 2022;586:152753.
46. Johari N, Fathi MH, Golozar MA. The effect of fluorine content on the mechanical properties of poly (ϵ -caprolactone)/nano-fluoridated hydroxyapatite scaffold for bone-tissue engineering. *Ceramics International*. 2011;37(8):3247-51.
47. Wang J, Chao Y, Wan Q, Zhu Z, Yu H. Fluoridated hydroxyapatite coatings on titanium obtained by electrochemical deposition. *Acta Biomaterialia*. 2009;5(5):1798-807.